All-Optical Measurement-Based Quantum-Information Processing in Quantum Dots

Avinash Kolli,[1,*] Brendon W. Lovett,[1,†] Simon C. Benjamin,[1] and Thomas M. Stace[2]

[1]*Department of Materials, Oxford University, Oxford OX1 3PH, United Kingdom*

[2]*DAMTP, University of Cambridge, Cambridge, CB3 0WA, United Kingdom*

(Received 5 July 2006; published 22 December 2006)

Parity measurements on qubits can generate the entanglement resource necessary for scalable quantum computation. Here we describe a method for fast optical parity measurements on electron spin qubits within coupled quantum dots. The measurement scheme, which can be realized with existing technology, consists of the optical excitation of excitonic states followed by monitored relaxation. Conditional on the observation of a photon, the system is projected into the odd/even-parity subspaces. Our model incorporates all the primary sources of error, including detector inefficiency, effects of spatial separation and nonresonance of the dots, and also unwanted excitations. Through an analytical treatment we establish that the scheme is robust to such effects. Two applications are presented: a realization of a controlled-NOT gate, and a technique for growing large scale graph states.

DOI: 10.1103/PhysRevLett.97.250504 PACS numbers: 03.67.Lx, 71.35.Pq, 73.20.Mf, 78.67.Hc

Quantum computation (QC) offers the possibility of exponential speedup over classical computation [1]. Many of the ideas put forward for implementing QC in the solid state involve using electron spins to represent qubits. In order to create controlled entanglement these schemes typically envisage some mechanism for switching on and off spin-spin interactions [2]. This is an enormous challenge experimentally. Recently, Beenakker *et al.* [3] have shown that it is possible to use parity measurements on pairs of spins rather than interaction switching. Together with single spin rotations, such measurements suffice to implement scalable QC. A scheme for exploiting this idea in the solid state with electrostatically defined dots has been advanced by Engel and Loss [4]; while Barrett and Stace [5] propose a similar scheme for a spin singlet-triplet measurement. These ideas rely on charge detection and therefore require electrode structures in the vicinity of the qubits. Here we consider an alternative optical measurement of spin parity that can be implemented in quantum-dot (QD) structures.

The optical process involves the excitation of odd-parity spin states to higher excitonic states. The readout is achieved by the radiative relaxation of these excited states, and then the observation of a photon which projects the system into the odd-parity subspace. Conversely, when no photon is observed the system is projected into the even-parity subspace. Since any additional single qubit gates can also be implemented through optical pulses [6], this scheme constitutes an all-optical approach to measurement-based QC in the solid state.

Model.—Consider two QDs, each of which are n doped so that they each contain an excess conduction band electron. The qubit basis $|0\rangle$ and $|1\rangle$ is defined by the electron spin states $m_z = -1/2$ and $1/2$, respectively. We consider subjecting the structure to a single laser radiating both QDs with σ^+ polarized light. By the Pauli blocking effect, the creation of an exciton is possible only for the $|m_z = 1/2\rangle$ state [7]. This exciton-spin (trion) state is denoted as $|X\rangle$.

The Hamiltonian for our two quantum dots driven by a classical laser field is

$$H(t) = \omega_a|X\rangle\langle X| \otimes \hat{I} + \omega_b \hat{I} \otimes |X\rangle\langle X| + V_{XX}|XX\rangle\langle XX| + V_F(|1X\rangle\langle X1| + \text{H.c.}) + \Omega \cos\omega_l t(|1\rangle\langle X| \otimes \hat{I} + \hat{I} \otimes |1\rangle\langle X| + \text{H.c.}), \quad (1)$$

where H.c. denotes Hermitian conjugate and ω_a and ω_b are the exciton creation energies for dot a and dot b, respectively. V_F is the strength of the Foerster interaction, which causes exciton transfer between the dots via virtual photon exchange. V_{XX} is the biexcitonic energy shift due to the exciton-exciton dipole interaction, Ω is the time-dependent laser coupling (assumed to be the same for both dots), and ω_l is the laser frequency. The energy difference between the $|0\rangle$ and $|1\rangle$ states is negligible on the exciton energy scale. The Foerster interaction is nonmagnetic and couples only states $|X1\rangle$ and $|1X\rangle$. We first consider resonant dots such that $\omega_a = \omega_b = \omega_0$ (see Fig. 1).

The Hamiltonian (1) may be decoupled into three subspaces with no interactions between them: $\mathcal{H}_0 = \{|00\rangle\}$, $\mathcal{H}_1 = \{|01\rangle, |0X\rangle, |10\rangle, |X0\rangle\}$, $\mathcal{H}_2 = \{|11\rangle, |X1\rangle, |X1\rangle, |XX\rangle\}$. Let us look at the Hamiltonian for the last of these subspaces. We write this in a basis of the eigenstates for $\Omega = 0$, which are $|11\rangle$, $|\psi_+\rangle = (1/\sqrt{2})(|1X\rangle + |X1\rangle)$, $|\psi_-\rangle = (1/\sqrt{2})(|1X\rangle - |X1\rangle)$, and $|XX\rangle$. The degeneracy of the $|\psi_-\rangle$ and $|\psi_+\rangle$ levels is lifted by the Foerster interaction, resulting in two states each containing a delocalized exciton. In this basis

$$H_2 = (\omega_0 + V_F)|\psi_+\rangle\langle\psi_+| + (\omega_0 - V_F)|\psi_-\rangle\langle\psi_-| + (2\omega_0 + V_{XX})|XX\rangle\langle XX| + \Omega' \cos\omega_l t(|11\rangle\langle\psi_+| + |\psi_+\rangle\langle XX| + \text{H.c.}), \quad (2)$$

where $\Omega' = \Omega\sqrt{2}$.

We achieve our parity measurement by applying a π pulse tuned to the exciton creation energy ω_0, which will

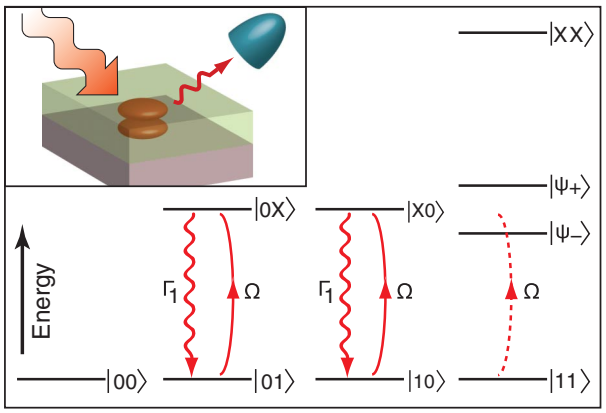

FIG. 1 (color online). Inset: schematic of a system suitable for a two-qubit demonstration. The double dot is subjected to an excitation pulse and monitored for photon emission (collection apparatus not shown). Main figure: energy level structure for two resonant dots, showing the operation of the parity measurement. The creation of excitons is possible only in the odd-parity subspace. The relaxation process in the odd-parity subspace results in the emission of a photon which is subsequently detected.

populate the $|0X\rangle$ and $|X0\rangle$ states fully, while the $|00\rangle$ and $|11\rangle$ states remain as they are owing to the Foerster splitting (see Fig. 1). Next we allow the system to relax: if we measure a photon without determining from which QD it originated, we expect the state of the system to be projected into the spin-parity odd subspace while retaining the initial coherence between the $|01\rangle$ and $|10\rangle$ states. If no photon is measured, then we expect that the system will collapse into the even-parity subspace, again retaining the necessary coherence for the parity measurement.

For perfect fidelity of operation we need to ensure that after the initialization procedure there is no population of the $|\psi_+\rangle$ and $|XX\rangle$ states. Returning to the Hamiltonian for the $\mathcal{H}_2$ subspace [Eq. (2)], moving into a frame rotating at frequency $\omega_l = \omega_0$ and making a rotating wave approximation, we may write

$$H_2 = -V_F|\psi_-\rangle\langle\psi_-| + V_F|\psi_+\rangle\langle\psi_+| + V_{XX}|XX\rangle\langle XX| + \Omega'/2(|11\rangle\langle\psi_+| + |\psi_+\rangle\langle XX| + \text{H.c.}). \quad (3)$$

Under the conditions $|V_F|, |V_{XX}| \gg |\Omega'|/2$ the $|11\rangle \leftrightarrow |\psi_+\rangle$ and $|\psi_+\rangle \leftrightarrow |XX\rangle$ transitions are suppressed.

We use the quantum trajectories formalism to analyze the dynamics of our measurement process. As described in [8,9] the conditional master equation (CME) for a system with n imperfect measurement channels is

$$d\rho_c = -i[H,\rho_c]dt + \sum_{j=1}^{n}\left\{[\eta_j \mathrm{Tr}(\mathcal{J}[c_j]\rho_c)\rho_c + (1-\eta_j)\mathcal{J}(c_j) - \mathcal{A}(c_j)\rho_c]dt + \left(\frac{\mathcal{J}[c_j]\rho_c}{\mathrm{Tr}(\mathcal{J}[c_j]\rho_c)} - \rho_c\right)dN_j\right\}, \quad (4)$$

where ρ_c is the density matrix of the system, H is the system Hamiltonian in the interaction picture, c_j is the Lindblad operator through which the system couples to the measurement channel j, $\mathcal{J}[c_j]$ is the jump operator which projects out the component of the state that is consistent with a detection in channel j and is defined as $\mathcal{J}[c_j]\rho_c = c_j^\dagger \rho_c c_j$. $\mathcal{A}[c_j]$ is defined as $\mathcal{A}[c_j]\rho_c = \frac{1}{2} \times (c_j^\dagger c_j \rho_c + \rho_c c_j^\dagger c_j)$, η_j is the efficiency of detector channel j and dN_j is the classical stochastic increment taking the values $\{0, 1\}$ and denotes the number of photons detected from channel j in the interval t, $t + dt$. Equation (4) is equivalent to the linear, unnormalized, CME

$$\dot{\tilde{\rho}} = -i[H,\tilde{\rho}] + \sum_{j}^{n}\{(1-\eta_j)\mathcal{J}[c_j]\tilde{\rho} - \mathcal{A}[c_j]\tilde{\rho}\}, \quad (5)$$

where $\rho_c = \tilde{\rho}/\mathrm{Tr}(\tilde{\rho})$.

For coupling strengths satisfying the criteria following Eq. (3), we are able to consider only one coupling channel describing the continuous measurement process. This coupling channel describes the radiative decay of the excited states in the odd-parity subspace. The coupling operator is taken to be of the form $c_1 = \sqrt{\Gamma_1}(|10\rangle\langle X0| + |01\rangle\langle 0X|)$, where $\sqrt{\Gamma_1}$ is the decay rate for a single exciton, and the detector efficiency is η_1. This form of the Lindblad operator ensures that the measurement does not distinguish photons originating from different dots which, as we show later, is reasonable for sufficiently close QDs.

We define the fidelity of the measurement, conditional on not measuring a photon, as $F_0 = \langle\psi_E|\rho_f|\psi_E\rangle$ where ρ_f is the state of the system at the end of the measurement and the target state is $|\psi_E\rangle = \alpha_{00}|00\rangle + \alpha_{11}|11\rangle$. Meanwhile, the fidelity conditional on measuring the photon at time t is $F_1(t) = \langle\psi_O|\rho(t)|\psi_O\rangle$ with target state $|\psi_O\rangle = \alpha_{01}|01\rangle + \alpha_{10}|10\rangle$.

We solve the CME analytically for our simple model, with the state initially in an equal superposition of all four computational basis states. The probability p_{even} that at a time t we are in the even subspace conditioned on not observing a photon is $p_{\mathrm{even}}(t) = [2 + \eta_1(e^{-\Gamma_1 t} - 1)]^{-1}$, while, on measuring a photon the probability that we have collapsed into the odd space $p_{\mathrm{odd}}(t)$ is unity, as expected. The probability $p_{\mathrm{even}}(t)$ is plotted in Fig. 2 as a function of t and η_1. Other parameters are set to typical values: $V_F = 0.85$ meV, $V_{XX} = 5$ meV, $\omega_0 = 2$ eV, $\Omega = 0.1$ meV, and $\Gamma_1 = 4\ \mu$eV [10–13].

After 10 ns the probability of photon emission is negligible, and there is essentially no further evolution beyond this time. This sets a characteristic time scale for the measurement process. At this time if no photon has been measured we obtain a fidelity of $F_0 = (2 - \eta_1)^{-1}$. Realistically, the losses at various stages in the detection procedure give rise to a photon detection efficiency of 50% [14]; a value that will be used throughout the rest of this Letter. To boost the fidelity we can repeat the excite-decay procedure several times. Every additional cycle wherein no

photon is detected increases our confidence that the state is in the even-parity subspace. The fidelity after n excite-decay cycles is $F_0^n = [1 + (1 - \eta)^n]^{-1}$.

We have shown above that on detection of a photon, we obtain a perfect fidelity for our parity measurement. However, we have up to this point neglected a number of effects that may reduce the performance of our measurement. For example, we have ignored the effects of excitations to the $|\psi_+\rangle$ and $|XX\rangle$ states. We have also ignored two possible ways in which the QDs could be distinguished when a photon is detected, namely, spatial separation and nonresonance of the QDs.

To analyze the effect of spatial separation we derive the CME from first principles, starting from the microscopic Hamiltonian: $H_{\rm tot} = \omega_0(c_A^\dagger c_A + c_B^\dagger c_B) + \sum_k \omega_k a_k^\dagger a_k + H_I$, where

$$H_I = \sum_{\mathbf{k}} (\mu.\hat{\sigma}_{\mathbf{k}})\epsilon_{\mathbf{k}} a_{\mathbf{k}} e^{i\mathbf{k}.\mathbf{r}}(c_A^\dagger + e^{i\mathbf{k}.\Delta\mathbf{r}} c_B^\dagger) + \text{H.c.} \quad (6)$$

μ is the dipole moment vector for each qubit, $\hat{\sigma}_{\mathbf{k}}$ is the polarization vector for the electric field, $a_{\mathbf{k}}$ is the annihilation operator for a quantum of the electric field, $\mathbf{k}$ is the wave vector for the electric field, $c_{A,B}$ represents the annihilation operator for an exciton on dot A, B, respectively, and $\Delta\mathbf{r}$ is the center-to-center separation of the dots.

To proceed we iterate the Schrödinger equation twice to obtain an integrodifferential equation describing the evolution. Then we trace out the environmental degrees of freedom to obtain an unconditional master equation. Finally, we generate a CME by defining a jump operator describing the detection process. This yields the following:

$$\dot{\tilde{\rho}} = -i[H, \tilde{\rho}] + \sum_{\mathbf{k}} (1 - \eta_{\mathbf{k}}) P_{\mathbf{k}} \tilde{\rho} P_{\mathbf{k}}^\dagger - \{P_{\mathbf{k}}^\dagger P_{\mathbf{k}} \tilde{\rho} + \tilde{\rho} P_{\mathbf{k}}^\dagger P_{\mathbf{k}}\}, \quad (7)$$

where $P_{\mathbf{k}}^\dagger(r) = (\mu.\hat{\sigma}_{\mathbf{k}})\epsilon_{\mathbf{k}} e^{i\mathbf{k}.\mathbf{r}}(c_A^\dagger + e^{i\mathbf{k}.\Delta\mathbf{r}} c_B^\dagger)$. Summing over all the modes, we obtain

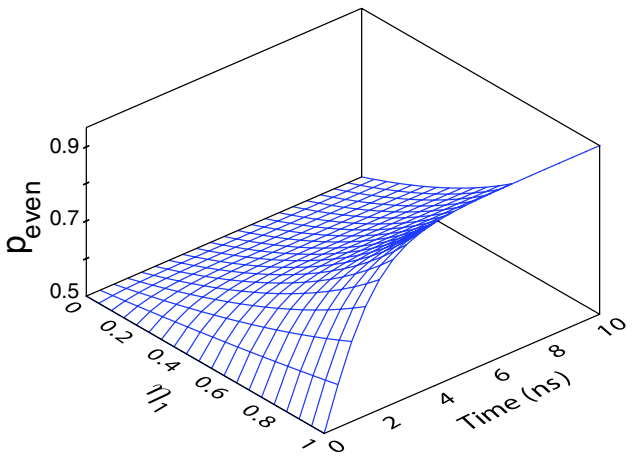

FIG. 2 (color online). Probability that the state is in the even-parity subspace $p_{\rm even}$ conditional on not measuring a photon.

$$\dot{\tilde{\rho}} = -i[H, \tilde{\rho}] + (1 - \eta)\mathcal{J}\tilde{\rho} - \mathcal{A}\tilde{\rho}, \quad (8)$$

where

$$\mathcal{J}\tilde{\rho} = \Gamma_1[c_A \rho c_A^\dagger + 3f(k_0\Delta r)(c_A \rho c_B^\dagger + c_B \rho c_A^\dagger) + c_B \rho c_B^\dagger],$$
$$\mathcal{A}\tilde{\rho} = \Gamma_1[c_A^\dagger c_A \rho + \rho c_A^\dagger c_A + c_B^\dagger c_B \rho + \rho c_B^\dagger c_B],$$
$$f(\alpha) = \frac{2\alpha\cos(\alpha) + (\alpha^2 - 2)\sin(\alpha)}{\alpha^3}. \quad (9)$$

Hence, the fidelity when a photon is detected is

$$F = \frac{1 + 3f(k_0\Delta r)}{2}. \quad (10)$$

In order for our scheme to work the Foerster interaction strength must be of order 1 meV [12], and this sets a value for Δr of 5 nm [12]. Using $\omega_0 = 2$ eV we obtain $k_0 = 10^7$ m^{-1}, and $k_0\Delta r = 5 \times 10^{-2}$. This leads to a modified fidelity of 0.999, and thus we conclude that our scheme is resilient to effects of spatial separation.

We now consider the situation of nonresonant QDs. If the detuning of the two transitions $\delta = \omega_a - \omega_b$ is large enough it will destroy the delocalization and resulting splitting due to the Foerster interaction, thus preventing selective excitation to states only in the odd subspace. Two inequalities must be satisfied: first, in order to excite excitons from both $|10\rangle$ and $|01\rangle$ with a single laser pulse, we require that $\delta \ll \Omega$. Second, to restrict transitions in the $\mathcal{H}_2$ subspace, we require that $\sqrt{\delta^2 + V_F^2}$, $V_{XX} \gg \Omega(b_2 \pm b_1)$ where $b_{1,2} = \sqrt{(A \mp 1)/2A}$ and $A = \sqrt{1 + (V_F^2/\delta^2)}$. These lead to the condition that $V_F \gg \delta$.

Returning to the effects of nonresonant dots on the relaxation process, we calculate a modified CME using the same method as used for the case of spatially separated dots. We obtain $c_1 = \sqrt{\Gamma_1}(c_A + e^{-i\delta t} c_B)$. Using this modified Lindblad operator in the CME we find that on measuring a photon the state of the system becomes

$$|\psi(t)\rangle = \alpha_{01}|01\rangle + \alpha_{10} e^{i\delta t}|10\rangle. \quad (11)$$

This extra phase is in general unknown and so is detrimental to the parity measurement, since it destroys the coherence between the states. However, accurate timing of the photon detection corrects for this; we can reverse the (now known) accumulated phase using single qubit phase gates that can be implemented optically [6]. State-of-the-art photon detectors have time resolutions of the order of picoseconds [15], so it is possible to correct for detunings of the order of 1 meV. This regime can be achieved with existing technology using an electric field to Stark shift the QDs on to resonance [16]. Alternatively, we could use molecular systems [17] which are identical and so the problem of nonresonance is effectively eliminated.

Finally, we consider the potential problem of excitations in the $\mathcal{H}_2$ subspace. To model these we allow a further two decay channels: $c_2 = \sqrt{\Gamma_2}|11\rangle\langle\psi_+|$ and $c_3 = \sqrt{\Gamma_3}|\psi_+\rangle \times \langle XX|$. The decay rates for these two channels are set by the

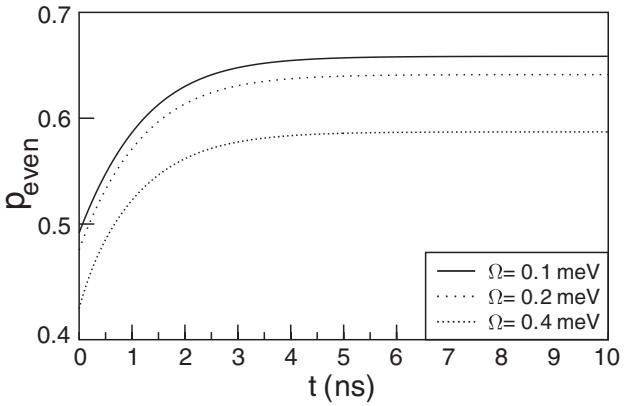

FIG. 3. p_{even} for various laser coupling strengths Ω when photons from $\mathcal{H}_2$ subspace are not detectable but simply lost to the environment.

dipole moments for the transitions. The allowed transitions within the $\mathcal{H}_2$ subspace have a larger dipole, hence $\sqrt{\Gamma_2} = \sqrt{\Gamma_3} = \sqrt{2\Gamma_1}$. We will assume that photons from these extra channels can be filtered out before they reach the detector. Numerical simulations for the probability that the system is in the even-parity subspace are presented in Fig. 3. Although there is some degradation in the performance, even for the strongest displayed laser coupling we obtain a final fidelity of over 0.5. This is sufficient to enable us to obtain extremely high fidelity using only a few rounds of the excite-decay procedure.

Spin relaxation effects (including electron-hole interactions) couple the subspaces and so might be a problem for our protocol. However, they occur on a time scale of the order of 20 ms [18], which can be ignored on the time scale of our measurement. Further, the electron spin-spin exchange interaction has been measured at less than 1 μeV in a quantum-dot system under a range of conditions [19]. This is considerably weaker than any other interactions present and can thus be safely neglected.

We have described a reliable method of performing a spin-parity measurement via the detection of a photon. Beenakker *et al.* suggested that this could be used to construct a CNOT gate by arranging two parity measurement gates in parallel. This is possible in a chain of three QDs if we have the ability to address two of the QDs with the laser while leaving the final QD unaffected. This may be achieved by using two different exciton transitions for the two different entangling gates.

The entangling procedure that we have described could be incorporated into a scheme to grow large scale graph states reliably [20]. Graph states are a certain type of multientangled state, which enable one to perform computational operations purely by performing single qubit measurements. A major difficulty with graph state computation comes from the successful preparation of the initial multientangled state. Benjamin *et al.* [20] propose a method of overcoming this in systems like the one discussed here, where a reliable method of entangling between pairs of qubits exists. Different pairs are then linked through any entangling process (that may be inefficient).

In conclusion, we have presented a novel scheme for implementing a spin-parity measurement on a pair of coupled quantum dots. We have estimated the fidelity of the parity measurement scheme presented here, and found it to be robust ($F > 95\%$) in the presence of realistic sources of errors, including inefficient photon detection, unwanted excitations in the $\mathcal{H}_2$ subspace, and spatial or spectral separation of the QDs. Finally, we identified two applications for our parity measurement: an implementation of a CNOT gate and a method of reliably constructing large scale graph states.

This work is supported by the QIPIRC (No. GR/S82176/01). B. W. L. is supported by DSTL and St. Anne's College, Oxford. B. W. L. and S. C. B. acknowledge support from the Royal Society.

*Electronic address: avinash.kolli@materials.ox.ac.uk
†Electronic address: brendon.lovett@materials.ox.ac.uk

[1] M. A. Nielsen and I. L. Chuang, *Quantum Computation and Quantum Information* (Cambridge University, Cambridge, U.K., 2000).
[2] B. E. Kane, Nature (London) **393**, 133 (1998).
[3] C. W. J. Beenakker, D. P. DiVincenzo, C. Emary, and M. Kindermann, Phys. Rev. Lett. **93**, 020501 (2004).
[4] H. Engel and D. Loss, Science **309**, 586 (2005).
[5] S. D. Barrett and T. M. Stace, Phys. Rev. B **73**, 075324 (2006).
[6] B. W. Lovett, New J. Phys. **8**, 69 (2006).
[7] E. Pazy *et al.*, Europhys. Lett. **62**, 175 (2003).
[8] T. M. Stace, G. J. Milburn, and C. H. W. Barnes, Phys. Rev. B **67**, 085317 (2003).
[9] C. W. Gardiner and P. Zoller, *Quantum Noise* (Springer, New York, 2000).
[10] D. Birkedal, K. Leosson, and J. M. Hvam, Phys. Rev. Lett. **87**, 227401 (2001).
[11] E. Biolatti, I. D'Amico, P. Zanardi, and F. Rossi, Phys. Rev. B **65**, 075306 (2002).
[12] B. W. Lovett, J. H. Reina, A. Nazir, and G. A. D. Briggs, Phys. Rev. B **68**, 205319 (2003).
[13] P. Borri *et al.*, Phys. Rev. Lett. **87**, 157401 (2001).
[14] W. L. Barnes *et al.*, Eur. Phys. J. D **18**, 197 (2002).
[15] PicoHarp 300, Time-Correlated Single Photon Counting System with USB interface user's manual and technical data (2005).
[16] A. Nazir *et al.*, Phys. Rev. B **71**, 045334 (2005).
[17] C. Hettich *et al.*, Science **298**, 385 (2002).
[18] M. Kroutvar *et al.*, Nature (London) **432**, 81 (2004).
[19] E. A. Laird *et al.*, Phys. Rev. Lett. **97**, 056801 (2006).
[20] S. C. Benjamin, D. E. Browne, J. Fitzsimons, and J. J. L. Morton, New J. Phys. **8**, 141 (2006).